Spherical Light Integration over Spherical Caps via Spherical Harmonics

Zihong Zhou, Li-Yi Wei

Spherical Light Integration over Spherical Caps via Spherical Harmonics

Zihong Zhou
South China Agricultural University

Li-Yi Wei
Adobe Research

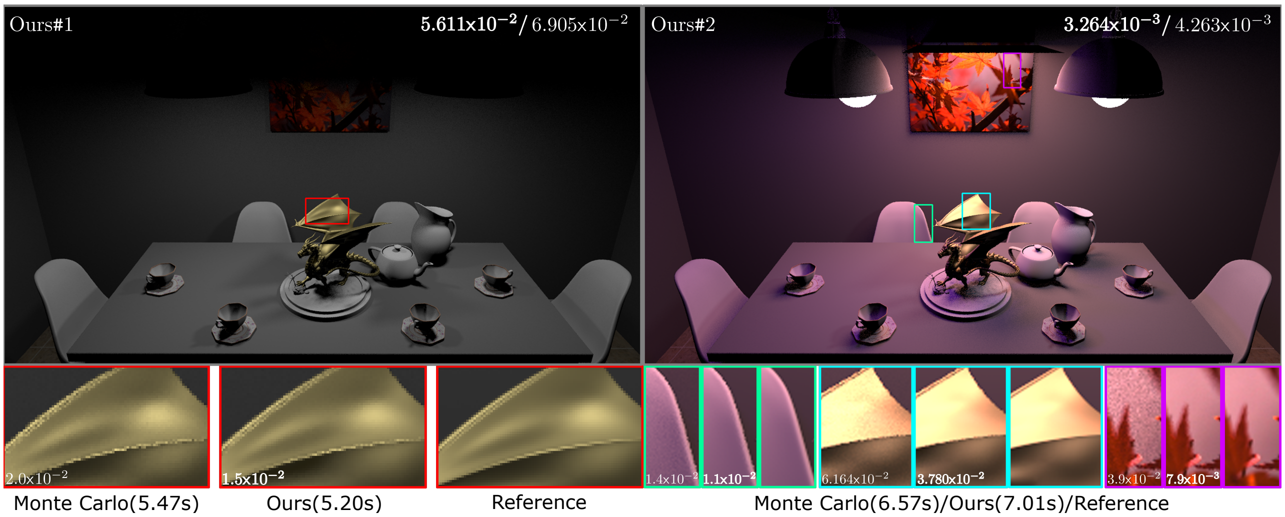

Figure 1: *Equal time comparison of Monte Carlo rendering and our method.* This dining room scene is lit by 2 sphere lights (left) and 1 quad light (right). Our method uses order 16 SH expansions for the rough gold BRDF (highlighted on the left) and order 8 for diffuse BRDF. We compare relative MSE numbers for full image (top) and several insets (bottom). Our method can outperform Monte Carlo sampling (MIS) method for direct lighting with good approximation of low frequency BRDF.

ABSTRACT

Spherical area light sources are widely used in synthetic rendering. However, traditional Monte Carlo methods can require an excessive number of samples for sufficient accuracy. We propose a Spherical Harmonics (SH) based method to provide a trade-off between performance and accuracy. Our key idea is an analytical integration of SH over spherical caps. The SH integration is first decomposed into a weighted sum of Zonal Harmonics (ZH) integration, which could be evaluated using recurrence formulae. The resulting integration could then be used for rendering spherical area lights efficiently, saving 50% light samples at best while maintaining competitive accuracy. Our method can easily fit into an existing SH based rendering framework to support near-field sphere lighting.

CCS CONCEPTS

• **Computing methodologies** → **Rendering**.

KEYWORDS

ray tracing, area lighting, spherical harmonics

ACM Reference Format:

Zihong Zhou and Li-Yi Wei. 2020. Spherical Light Integration over Spherical Caps via Spherical Harmonics. In *SIGGRAPH Asia 2020 Technical Communications (SA '20 Technical Communications), December 4–13, 2020, Virtual Event, Republic of Korea.* ACM, New York, NY, USA, 4 pages. https://doi.org/10.1145/3410700.3425427

1 INTRODUCTION

Spherical cap integration is ubiquitous in rendering. Area lighting for example, an essential component in a production renderer for generating photorealistic images, requires solving the direct illumination integral [Wang 1992] or rendering equation [Kajiya 1986]. However, finding a closed-form solution to these integrals remains a challenging problem. Numerical integration algorithms such as Monte Carlo sampling could be used to solve the integral, but the process demanding possibly massive number of samples to converge might result in low performance.

There have been active research projects focusing on sampling [Arvo 1995b, 2001; Gamito 2016; Guillén et al. 2017; Peters and Dachsbacher 2019; Ureña et al. 2013; Ureña and Georgiev 2018] to reduce variance and improve convergence rate. On the other hand, solutions based on closed-form integration leveraging spherical distribution approximation have been proposed [Dupuy et al. 2017;

SA '20 Technical Communications, December 4–13, 2020, Virtual Event, Republic of Korea

ACM ISBN 978-1-4503-8080-5/20/11…$15.00
https://doi.org/10.1145/3410700.3425427

Heitz et al. 2016] recently. However, various types of BRDFs featuring distinctive characteristics might be difficult to fit with these specific spherical distributions.

Spherical Harmonics (SH) provide another way to efficiently project and reconstruct spherical integrand in many cases, which could be used for shading complex BRDF with area light [Ramamoorthi and Hanrahan 2001; Sloan et al. 2002]. However, this requires an efficient estimation of spherical integrals via SH expansion. Fortunately, the SH expansion integration over spherical polygon could be solved via *axial moments* [Arvo 1995a; Belcour et al. 2018] and optimized by Zonal Harmonics (ZH) recurrence [Wang and Ramamoorthi 2018]. In order to support spherical luminaries, we extend the recurrence formulae to handle clipped spherical cap integration, a more efficient method compared to adapting [Snyder 1996]'s monomial recurrence.

2 BACKGROUND

Direct Illumination Integral. The contributed radiance at p along direction ω_o of area light could be expressed as [Wang 1992]:

$$L_o(p, \omega_o) = \int_{\Omega} f(p, \omega_o, \omega_i) L_d(p, \omega_i) |\omega_i \cdot n| \, \mathrm{d}\omega_i \tag{1}$$

, where Ω is the subtended solid angle, f is Bidirectional Reflection Distribution Function (BRDF), L_d is the emitted radiance at ω_i and $|\omega_i \cdot n|$ is the cosine factor.

Spherical Harmonics Expansions for Direct Lighting. The real spherical harmonics (SH) in spherical coordinates are:

$$y_l^m(\theta, \phi) = K_l^m P_l^{|m|}(\cos\theta) f(|m|\phi) \tag{2}$$

, where $K_l^m = \sqrt{\frac{(2l+1)}{4\pi} \frac{(l-|m|)!}{(l+|m|)!}}$, P_l^m are the associate Legendre polynomials and $f(|m|\phi)$ is 1 for $m = 0$, $\sqrt{2}\cos(m\phi)$ for $m > 0$ and $\sqrt{2}\sin(|m|\phi)$ for $m < 0$.

We could project $L_d(p, \omega_i)$ and $f(p, \omega_o, \omega_i)|\omega_i \cdot n|$ onto SH bases yielding SH coefficients:

$$f_l^m(p, \omega_o) = \int_{\Omega} f(p, \omega_o, \omega_i) |\omega_i \cdot n| y_l^m(\omega_i) \, \mathrm{d}\omega_i \tag{3}$$

$$L_l^m(p, \omega_o) = \int_{\Omega} L_d(p, \omega_i) y_l^m(\omega_i) \, \mathrm{d}\omega_i \tag{4}$$

Direct lighting integral could thus be expanded via orthogonality of SH functions:

$$L_o(p, \omega_o) \approx \sum_{l=0}^{n-1} \sum_{m=-l}^{l} f_l^m(p, \omega_o) L_l^m(p, \omega_o) \tag{5}$$

There are analytical solutions to the light coefficients $L_l^m(p, \omega_o)$ for near-field polygonal area lights while $f_l^m(p, \omega_o)$ are usually precomputed by numerical methods.

Zonal Harmonics Factorization. A spherical harmonics (SH) could be expressed by a weighted sum of rotated zonal harmonics (ZH) via *Zonal Harmonics Factorization* [Nowrouzezahrai et al. 2012]:

$$y_l^m(\omega_i) = \sum_{\bar{m}=-l}^{l} \alpha_{l,\bar{m}}^m y_l^0(\omega_i \to \omega_d) \tag{6}$$

, where ZH function $y_l^0(\omega)$ is simply a subset of SH function ($m = 0$), $y_l^0(\omega_i \to \omega_d)$ is the ZH function rotated to ω_d direction, evaluated at ω_i and $\alpha_{l,\bar{m}}^m$ are related weighting coefficients.

Assuming a constant L_d, Equation (4) could be expressed as an integral of Legendre polynomials via

$$y_l^0(\omega_i \to \omega_d) = \sqrt{\frac{2l+1}{4\pi}} P_l(\omega_i \to \omega_d) \tag{7}$$

$$L_l^m(p, \omega_o) = \sqrt{\frac{2l+1}{4\pi}} L_d \sum_{\bar{m}=-l}^{l} \alpha_{l,\bar{m}}^m \int_{\Omega} P_l(\omega_i \to \omega_d) \, \mathrm{d}\omega_i \tag{8}$$

, which could be expanded to a series of monomials [Arvo 1995a; Belcour et al. 2018] and solved analytically.

3 METHOD

In Section 3.1, we first apply the main recurrence formulae [Wang and Ramamoorthi 2018] to our surface integral. In Sections 3.2 and 3.3 we derive our novel recurrence formulae for integrating zonal harmonics over spherical caps.

3.1 Surface Integral Recurrence

Our goal is to seek an efficient and exact solution to L_l^m in Equation (8) over a spherical cap C:

$$S_l = \int_C P_l(\omega_i \to \omega_d) \, \mathrm{d}\omega_i = \int_{C'} P_l(z) \, \mathrm{d}\omega_i \tag{9}$$

, where C' is the spherical cap in our coordinate frame, aligning ω_d to Z-axis ($\mathbf{Z} = \omega_\mathbf{d}, \mathbf{Y} = \omega_\mathbf{d} \times \mathbf{L}, \mathbf{X} = \mathbf{Y} \times \mathbf{Z}$).

We apply the main recurrence formula from [Wang and Ramamoorthi 2018] which used Stokes' theorem and Legendre polynomial identity:

$$S_l = \frac{(l-2)(l-1)}{l(l+1)} S_{l-2} + \frac{2l-1}{l(l+1)} B_{l-1} \tag{10}$$

$$B_l = \oint_{\partial C'} P_{l-1}(z)(xdy - ydx) \tag{11}$$

3.2 Boundary Integral Recurrence

In this section, we derive our recurrence formula for boundary integral B_l, a contour integral over a spherical cap clipped by horizon. There are indeed two cases for the spherical boundary as illustrated in Figure 2 and could be unified by a partial contour (spherical arc) integral.

We first parametrize $\omega_\mathbf{i}$ as $\omega_\mathbf{i}(\phi) = \cos\sigma\mathbf{L} + \sin\sigma(\cos\phi\mathbf{L_1} + \sin\phi\mathbf{L_2})$ by an orthonormal basis $\{\mathbf{L}, \mathbf{L_1}, \mathbf{L_2}\}$:

$$\mathbf{L} = (\sin\theta, 0, \cos\theta), \mathbf{L_1} \equiv (\cos\theta, 0, -\sin\theta), \mathbf{L_2} \equiv (0, 1, 0) \tag{12}$$

B_l could be then written as:

$$\boxed{B_l = -\cos\sigma D_l + \cos\theta C_l} \tag{13}$$

, where we defined D_l and C_l as:

$$D_l = \int_{\phi_{\min}}^{\phi_{\max}} P_l(z) z \, \mathrm{d}\phi, C_l = \int_{\phi_{\min}}^{\phi_{\max}} P_l(z) \, \mathrm{d}\phi \tag{14}$$

, with symbols defined as $a = \cos\sigma\cos\theta, b = -\sin\sigma\sin\theta, z = a + b\cos\phi$.

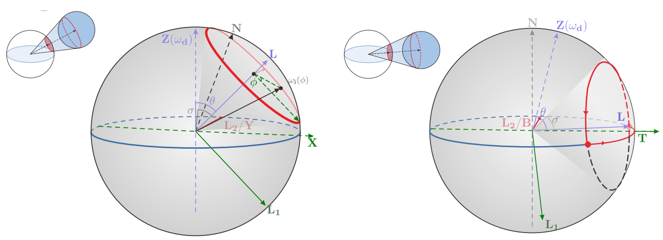

(a) Not clipped (b) Clipped

Figure 2: *Illustration of spherical light cap and geometric settings for integral derivation.* The ZH integral S_l over a spherical cap subtended by a spherical light source is converted to a single contour integral B_l for unclipped case in (a) and dual contour integrals B_{l1}, B_{l2} for clipped case in (b). Our spherical arc parametrization for $\omega_i(\phi)$ requires θ being the angle between L and ω_d and σ is the aperture angle of light cap.

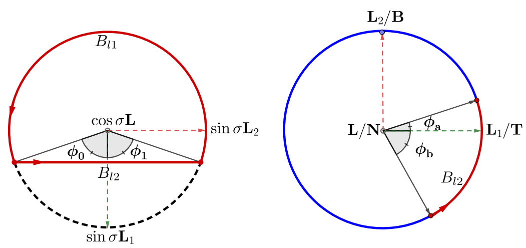

(a) Side view (b) Top view

Figure 3: *Side (a) and top (b) view of boundary integral B_l for integral limits in clipped case Figure 2b.* B_{l2} could be seen as a part of spherical cap contour where $\mathrm{L} = \mathrm{N}, \mathrm{L}_1 = \mathrm{T}, \mathrm{L}_2 = \mathrm{B}$.

By substitution of the Legendre polynomial identity, we reach the recurrence formula for C_l and D_l:

$$C_l = \frac{2l-1}{l} D_{l-1} - \frac{l-1}{l} C_{l-2} \tag{15}$$

$$\begin{aligned} D_l = \frac{1}{l+1} (&aC_l + lC_{l-1} + P_l(a + b\cos\phi_{\max})(b\sin\phi_{\max}) \\ &- P_l(a + b\cos\phi_{\min})(b\sin\phi_{\min}) \\ &+ (b^2 - a^2 - 1)E_l + 2aF_l) \end{aligned} \tag{16}$$

, where we defined E_l and F_l as:

$$E_l = \int_{\phi_{\min}}^{\phi_{\max}} \frac{\mathrm{d}P_l(z)}{\mathrm{d}z}\,\mathrm{d}\phi, F_l = \int_{\phi_{\min}}^{\phi_{\max}} \frac{\mathrm{d}P_l(z)}{\mathrm{d}z}\,\mathrm{d}\phi \tag{17}$$

The final recurrence formulae for E_l and F_l are obtained by substitution of another Legendre polynomial recurrence $P_l'(z) = (2l-1)P_{l-1}(z) + P_{l-2}'(z)$:

$$E_l = (2l-1)C_{l-1} + E_{l-2}, F_l = (2l-1)D_{l-1} + F_{l-2} \tag{18}$$

Clipped Spherical Cap. It is trivial to evaluate the unclipped case B_l letting $\phi_{\min} = 2\pi, \phi_{\max} = 0$ (for positive orientation) while the second case, clipped spherical boundary is decomposed via $B_l = B_{l1} + B_{l2}$. B_{l1} is addressed by our general partial contour integral above, where ϕ ranges from ϕ_0 to ϕ_1. The second contour curve B_{l2} is a part of horizon circumference, for which we parametrize $L = (0,0,1)$ with $\sigma = \frac{\pi}{2}, \theta = \cos^{-1}(\omega_d \cdot (0,0,1))$ and integral limit ϕ_a and ϕ_b.

Integral Limits. The integral limits ϕ_0, ϕ_1 could be computed by finding the intersection of spherical arc and tangent plane as shown in Figure 3. They are solutions to the equation $X_z\omega_{ix} + Y_z\omega_{iy} + Z_z\omega_{iz} = 0$:

$$\boxed{\phi_0 = \cos^{-1}(\frac{d}{c'}) - \varphi \quad \phi_1 = 2\pi - \cos^{-1}(\frac{d}{c'}) - \varphi} \tag{19}$$

$$\begin{aligned} &a' = \sin\sigma(X_z\cos\theta - Z_z\sin\theta) \quad d = -\cos\sigma(Z_z\cos\theta + X_z\sin\theta) \\ &b' = Y_z\sin\sigma \quad c' = \sqrt{a'^2 + b'^2} \quad \varphi = \tan^{-1}(\frac{-b'}{a}) \end{aligned} \tag{20}$$

ϕ_a and ϕ_b could be solved in the same manner as ϕ_0 and ϕ_1 as if we have done in Section 3.2 for clipped spherical cap case.

3.3 Initial Conditions

Iterative evaluation of our recurrence formulae in Equations (11), (15), (16) and (18) requires respective initial conditions. Intermediate boundary integrals $B_0, B_1, C_0, C_1, D_0, D_1, E_0, E_1, F_0, F_1$ are elementary definite integrals while the surface integral S_0, S_1 is a bit intricate. Note that S_0 is the solid angle of the clipped spherical cap and has the analytic solution from [Oat and Sander 2006]:

$$S_0 = \begin{cases} 2\pi(1-\cos\sigma), & \frac{\pi}{2} - \sigma \geq \cos^{-1}(L_z) \\ 0, & \sigma + \frac{\pi}{2} \leq \cos^{-1}(L_z) \\ 2\pi - 2\pi\cos\sigma - 2\cos^{-1}(\frac{L_z}{\sin\sigma}) & \\ +\frac{2\cos\sigma\cos^{-1}(\cos\sigma L_z)}{\sin\sigma\sin(\cos^{-1}(L_z))}, & \text{otherwise} \end{cases} \tag{21}$$

S_1 corresponds to the irradiance over spherical cap and could be converted to boundary integral B_0 by Stokes' theorem [Snyder 1996]:

$$S_1 = \int_{C'} z\,\mathrm{d}\omega_i = \frac{1}{2}\oint_{\partial C'}(xdy - ydx) = \frac{1}{2}B_0 \tag{22}$$

4 RESULTS

We experiment with our method on an OptiX [Parker et al. 2010] based GPU ray tracer, running at GTX 1060. We tabulate BRDF coefficients f_l^m and compute light coefficients L_l^m on the fly, using Equation (5) to compute direct lighting. Shadowing is achieved by control variates method [Heitz et al. 2018] with Monte Carlo sampling.

In Figure 1, we achieve complex lighting from multiple area lights simply by adding L_l^m from spherical caps (via our method) and polygon domains (via [Wang and Ramamoorthi 2018]). An accuracy validation of our method against MC integration is given in Figure 5, indicating that ours efficiently reduces variance at low sampling rate. In Figure 6 we compare our polynomial recurrence with monomial recurrence [Snyder 1996] for computing B_l in Section 3.2, where timings are measured by rendering Figure 5 with 1spp. Finally, we apply to measured BRDF from UTIA database [Filip and Vavra 2014] in Figure 4.

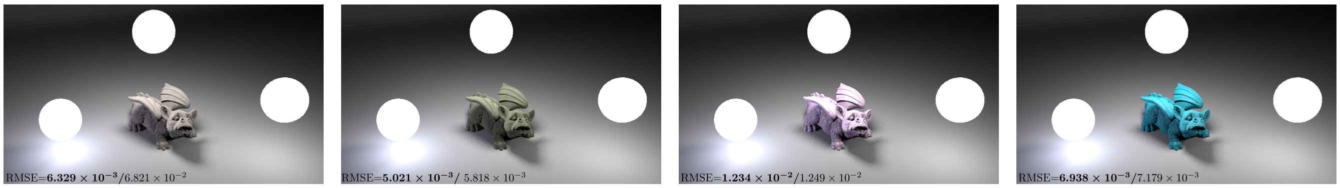

(a) Corduroy **(b) Carpet** **(c) Fabric1** **(d) Fabric2**

Figure 4: ***Rendering of several measured BRDFs [Filip and Vavra 2014] lit by three spherical lights using our method.*** **For all scenes: we use order 16 expansions and 96 samples for our method (6s) and 192 samples (accounting for light samples and shadow samples) for Monte Carlo sampling with MIS (5.8s).**

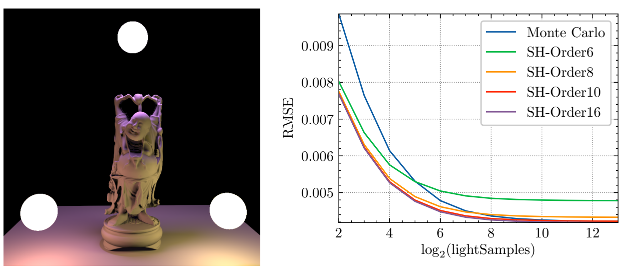

(a) Rendering **(b) Convergence plot**

Figure 5: ***Accuracy comparison of our method with MC integration using different SH orders.*** **In this case, order 10 SH expansion has already provided good approximation while being efficient (0.75x slower than MC).**

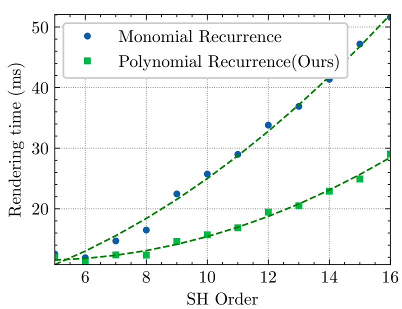

Figure 6: ***Performance plot of our method and [Snyder 1996] in rendering Figure 5a with different SH orders.*** **Our Legendre polynomial recurrence is more efficient and has better scalability than expanding to a series of monomials [Snyder 1996] despite enabling full compiler optimization.**

5 LIMITATIONS AND FUTURE WORK

Spherical harmonics provide an efficient way to expand low frequency spherical integrands, enabling us to solve many interesting problems in rendering. We address near-field spherical area lighting by extending [Wang and Ramamoorthi 2018]'s recurrence formulae for zonal harmonics to (clipped) spherical cap domains. For future work, we would like to generalize our method to more types of emissive geometries (e.g. disk and ellipsoid) and textures.

REFERENCES

James Arvo. 1995a. Applications of Irradiance Tensors to the Simulation of Non-Lambertian Phenomena. In *SIGGRAPH '95*. 335–342.

James Arvo. 1995b. Stratified sampling of spherical triangles. In *SIGGRAPH '95*. 437–438.

James Arvo. 2001. Stratified sampling of 2-manifolds. *SIGGRAPH 2001 Course Notes* 29, 2 (2001).

Laurent Belcour, Guofu Xie, Christophe Hery, Mark Meyer, Wojciech Jarosz, and Derek Nowrouzezahrai. 2018. Integrating Clipped Spherical Harmonics Expansions. *ACM Trans. Graph.* 37, 2, Article Article 19 (2018), 12 pages.

Jonathan Dupuy, Eric Heitz, and Laurent Belcour. 2017. A Spherical Cap Preserving Parameterization for Spherical Distributions. *ACM Trans. Graph.* 36, 4, Article Article 139 (2017), 12 pages.

Jiří Filip and R. Vavra. 2014. Template-Based Sampling of Anisotropic BRDFs. *Computer Graphics Forum* 33 (2014), 91–99.

Manuel N Gamito. 2016. Solid angle sampling of disk and cylinder lights. In *Computer Graphics Forum*, Vol. 35. Wiley Online Library, 25–36.

Ibón Guillén, Carlos Ureña, Alan King, Marcos Fajardo, Iliyan Georgiev, Jorge López-Moreno, and Adrian Jarabo. 2017. Area-Preserving Parameterizations for Spherical Ellipses. In *Computer Graphics Forum*, Vol. 36. 179–187.

Eric Heitz, Jonathan Dupuy, Stephen Hill, and David Neubelt. 2016. Real-Time Polygonal-Light Shading with Linearly Transformed Cosines. *ACM Trans. Graph.* 35, 4, Article Article 41 (2016), 8 pages.

Eric Heitz, Stephen Hill, and Morgan McGuire. 2018. Combining analytic direct illumination and stochastic shadows. In *I3D '18*. 1–11.

James T. Kajiya. 1986. The Rendering Equation. In *SIGGRAPH '86*. 143–150.

Derek Nowrouzezahrai, Patricio Simari, and Eugene Fiume. 2012. Sparse zonal harmonic factorization for efficient SH rotation. *ACM Transactions on Graphics (TOG)* 31, 3 (2012), 1–9.

Chris Oat and Pedro Sander. 2006. Ambient Aperture Lighting. In *ACM SIGGRAPH 2006 Courses (SIGGRAPH '06)*. 143–152.

Steven G. Parker, James Bigler, Andreas Dietrich, Heiko Friedrich, Jared Hoberock, David Luebke, David McAllister, Morgan McGuire, Keith Morley, Austin Robison, and Martin Stich. 2010. OptiX: A General Purpose Ray Tracing Engine. , Article 66 (2010), 13 pages.

Christoph Peters and Carsten Dachsbacher. 2019. Sampling Projected Spherical Caps in Real Time. *Proceedings of the ACM on Computer Graphics and Interactive Techniques* 2, 1 (2019), 1–16.

Ravi Ramamoorthi and Pat Hanrahan. 2001. An Efficient Representation for Irradiance Environment Maps. In *SIGGRAPH '01*. 497–500.

Peter-Pike Sloan, Jan Kautz, and John Snyder. 2002. Precomputed Radiance Transfer for Real-Time Rendering in Dynamic, Low-Frequency Lighting Environments. In *SIGGRAPH '02*. 527–536.

John M Snyder. 1996. *Area light sources for real-time graphics.* Technical Report MSR-TR-96-11.

Carlos Ureña, Marcos Fajardo, and Alan King. 2013. An Area-Preserving Parametrization for Spherical Rectangles. In *EGSR '13*. Eurographics Association, Goslar, DEU, 59–66.

Carlos Ureña and Iliyan Georgiev. 2018. Stratified Sampling of Projected Spherical Caps. In *Computer Graphics Forum*, Vol. 37. 13–20.

Changyaw Wang. 1992. *Physically Correct Direct Lighting for Distribution Ray Tracing.* Academic Press Professional, Inc., 307–313.

Jingwen Wang and Ravi Ramamoorthi. 2018. Analytic Spherical Harmonic Coefficients for Polygonal Area Lights. *ACM Trans. Graph.* 37, 4, Article Article 54 (2018), 11 pages.